Vapor−Liquid−Liquid Equilibria of Hydrofluorocarbons + 1-Butyl-3-methylimidazolium Hexafluorophosphate

Mark B. Shiflett*,† and A. Yokozeki‡

DuPont Central Research and Development, Experimental Station, Wilmington, Delaware 19880, and DuPont Fluoroproducts Laboratory, Chestnut Run Plaza 711, Wilmington, Delaware 19880

In recent reports, we measured the vapor−liquid−liquid equilibria (VLLE) of trifluoromethane (R-23) and pentafluoroethane (R-125) with a room-temperature ionic liquid (RTIL), 1-butyl-3-methylimidazolium hexafluorophosphate [bmim][PF_6], using a volume−mass measurement method along various isotherms. In the present work, we complete similar investigation of VLLE for the methane and ethane series of hydrofluorocarbons (HFCs) in [bmim][PF_6]. Compounds studied here are fluoromethane (R-41), 1,1,1,2-tetrafluoroethane (R-134a), 1,1,1-trifluoroethane (R-143a), 1,1-difluoroethane (R-152a), and fluoroethane (R-161) in [bmim][PF_6]. Observed VLLE behaviors are consistent with the earlier predictions by our equation-of-state (EOS) model, which showed partial immiscibilities in the HFC-rich side solutions, indicating type-III or type-V mixtures according to the Konynenburg−Scott classification. Thus, the present study as well as those with R-23 and R-125 reasonably validate our EOS model. In addition, very large negative excess molar volumes have been observed for all the studied systems, similar to that observed for mixtures with R-23 and R-125.

Introduction

In our previous reports, we have shown that vapor−liquid equilibria (VLE) for hydrofluorocarbons (HFCs) and room-temperature ionic liquids (RTILs) can be well-modeled with both the modified Redlich−Kwong equation-of-state (EOS)[1−4] and activity (solution) models.[5−7] However concerning the vapor−liquid−liquid equilibria (VLLE) predictions based on the VLE data alone, it has been found that our EOS model can be more reliable than those activity models. Indeed, our recent studies on VLLE with a lower critical solution temperature (LCST) for trifluoromethane (R-23) and pentafluoroethane (R-125) in 1-butyl-3-methylimidazolium hexafluorophosphate, [bmim][PF_6][2,3] confirmed our EOS model calculations. The purpose of the present paper is to complete our study of HFCs by measuring VLLE for fluoromethane (R-41), 1,1,1,2-tetrafluoroethane (R-134a), 1,1,1-trifluoroethane (R-143a), 1,1-difluoroethane (R-152a), and fluoroethane (R-161) in [bmim][PF_6] and to confirm further our EOS model predictions. Here, it should be mentioned that in the case of R-32 (difluoromethane) and R-134 (1,1,2,2-tetrafluoroethane), our EOS model does not predict any VLLE behavior below the critical points of these compounds. Therefore, no quantitative VLLE analysis have been made for R-32 and R-134 mixtures, and only a brief discussion will be given.

In this work, we again employ our volumetric method[3] to determine directly VLLE properties of binary solutions including mole fractions and molar volumes of each liquid phase at a given temperature. The method is based only on volume−mass measurements of prepared sample containers without the use of any analytical instruments. We also confirm the phase boundary predictions using the well-established cloud-point measurement method.[8−16] The cloud-point temperature is an onset temperature for the heterogeneous liquid formation from a homogeneous liquid solution in a given binary composition. It is practically convenient and simple, but unlike the volumetric method, it only provides the composition of one of the liquid phases at the temperature; the composition of the other liquid phase must be estimated through the interpolation of many such observed phase-separation data.

First, we describe the principles of the present experimental method, which is a modification from that previously reported.[3] The analytical equations to solve the VLLE condition are more explicit and may provide another way to look at the volumetric method, although this does not necessarily give new information. Next, experimental details and results with error analyses are presented. The present VLLE data are compared with our EOS model predictions. Then, discussion and conclusions will follow.

Experimental Procedures

Principles of the Method. Here we use a modification of the method described in our previous work[3] to study the VLLE behavior of R-125 and [bmim][PF_6]. The present modified method provides analytical equations in more explicit forms to assist the readers in developing their own computer code. According to the Gibbs phase rule, VLLE of a binary system is a *univariant* state. This means that at a given intensive variable, say temperature, there is no freedom for other intensive variables. All other variables such as compositions, pressure, and densities of the system are uniquely determined regardless of any different extensive variables (volume of each phase and total mass of the system). The overall feed composition merely changes the physical volume in each phase, but the composition and density in each phase remains constant as long as the three phases exist at the fixed *T*.

This unique VLLE state of a binary system can be determined experimentally using a simple apparatus,[3] shown schematically in Figure 1, by mass-and-volume measurements *alone* without using any analytical method for the composition analysis. A

* Corresponding author. E-mail: mark.b.shiflett@usa.dupont.com.
† DuPont Central Research and Development.
‡ DuPont Fluoroproducts Laboratory.

10.1021/je060275f CCC: $30.25
Published on Web 08/15/2006

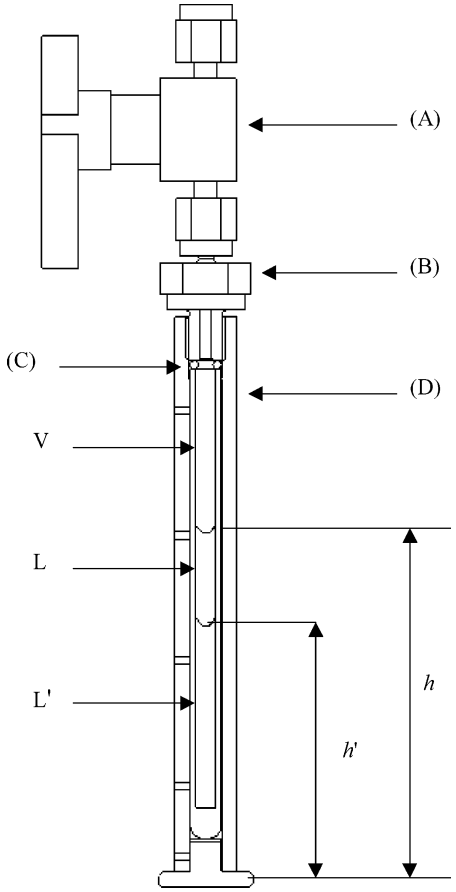

Figure 1. Schematic of the high-pressure experimental apparatus (L′, lower liquid phase; L, upper liquid phase; V, vapor phase; *h*′, height of lower liquid phase; *h*, height of upper liquid phase), (A) Swagelok valve (model SS-41GS2), (B) Swagelok fitting (SS-2-TA-1-OR), (C) Teflon O-ring, and (D) outer tube is polycarbonate shield, inner tube is borosilicate glass; see ref 3 for details.

set of mass-and-volume measurements of two sample containers at a constant temperature is sufficient to determine the required thermodynamic property.

The experimental procedure was as follows:

(1) A known amount of ionic liquid (compound I) was placed into the sample container (sample 0).

(2) The air was removed from the sample container. For low-pressure experiments or a small vapor-phase space in the container, air effects can be ignored.

(3) The mass of the ionic liquid was measured.

(4) A known amount of refrigerant (compound R) was added to sample 0, until two liquid phases appear.

(5) The mass increase in sample 0 was measured, which gives the amount of refrigerant. The refrigerant mass along with the ionic liquid mass measured in step 3 provided the initial overall feed composition (feed 0) of the container (sample 0).

(6) The sample container was kept at a constant *T*; wait a sufficient time for establishing the thermodynamic equilibrium.

(7) The volume of each phase (lower liquid phase, L′; upper liquid phase, L; and gas phase) was measured at a given constant *T*. Knowing the volume versus height calibration for the container, the height measurement of each phase will give the correct volumes of each phase.

(8) A second amount of refrigerant was added to sample 0, now called sample 1. In the case of refrigerant gas mixed with an ionic liquid, additional refrigerant can be added or removed. To remove refrigerant, carefully let some refrigerant leak out from the vapor space (mass of ionic liquid will not change due to it having a negligible vapor pressure). This along with steps 3 and 5 provided the final overall feed composition (feed 1) of the container (sample 1).

(9) Repeat steps 6 and 7.

An alternative approach to following steps 6 through 9, which can save time, was to prepare a second sample 1 simultaneously with the first sample 0.

(6a) Similarly, a second container (sample 1) was prepared, by repeating steps 1 to 5.

(7a) The two sample containers were kept at a constant *T*; wait a sufficient time for establishing the thermodynamic equilibrium.

(8a) The volume of each phase (upper liquid phase, L; lower liquid phase, L′; and gas phase) was measured at a given constant *T* for both sample containers.

With the above experimental data (masses and volumes), the VLLE condition can be determined, as shown below. The total moles of compound I in sample 0 (n_{IT0}) and sample 1 (n_{IT1}) are known from the measured mass and molecular weight of compound I in each container and the following relation holds:

$$n_{I0} + n_{I0}' = n_{IT0} \tag{1}$$

$$n_{I1} + n_{I1}' = n_{IT1} \tag{2}$$

where the subscripts I0 and I1 represent the compound I moles in liquid-phase L of the sample 0 and sample 1 containers, respectively; the ′ means the moles in liquid-phase L′. Molar volumes of the two liquids are unchanged (in the sample 0 and sample 1 containers) because VLLE of a binary system is a *univariant* state:

$$\frac{v_1}{v_0} = \frac{n_{R1} + n_{I1}}{n_{R0} + n_{I0}} \tag{3}$$

$$\frac{v_1'}{v_0'} = \frac{n_{R1}' + n_{I1}'}{n_{R0}' + n_{I0}'} \tag{4}$$

where the subscripts R0 and R1 mean compound R liquid moles in the sample 0 and sample 1 containers for the liquid-phase L, respectively; the ′ means the moles in liquid-phase L′. Subscripts (1 and 0) of the physical volume, *v*, correspond to the sample 0 and sample 1 containers for liquid-phase L, respectively, and the ′ means the volumes in the other liquid-phase L′.

Next, we observe that the mole fractions of the two liquids are unchanged in both containers because VLLE of a binary system is a *univariant* state:

$$\frac{n_{R0}}{n_{R0} + n_{I0}} = \frac{n_{R1}}{n_{R1} + n_{I1}} \tag{5}$$

$$\frac{n_{R0}'}{n_{R0}' + n_{I0}'} = \frac{n_{R1}'}{n_{R1}' + n_{I1}'} \tag{6}$$

Compound R total moles (n_{RT0} and n_{RT1}) in both containers are also known from the measured mass and molecular weight of compound *R* in each container and the following relation holds:

$$n_{R0} + n_{R0}' + n_{g0} = n_{RT0} \tag{7}$$

$$n_{R1} + n_{R1}' + n_{g1} = n_{RT1} \tag{8}$$

Gas-phase moles n_{g0} and n_{g1} for sample 0 and sample 1, respectively, can be obtained from the known gas volume, v_g,

and using an EOS[17] to calculate the vapor density. In most cases the refrigerant vapor can be assumed to be at the saturation condition; therefore, knowing only T, the vapor density can be calculated. For low-pressure fluids such as alcohols and water the contributions of n_{g0} and n_{g1} can be safely ignored; however, for high-pressure refrigerant gases the vapor phase moles must be included in the analysis.

The experimentally known quantities are n_{IT0}, n_{IT1}, n_{RT0}, n_{RT1}, n_{g0}, n_{g1}, v_1, v_0, v_1', v_0', and there are eight unknown parameters (n_{R0}, n_{I0}, n_{R1}, n_{I1}, n_{R0}', n_{I0}', n_{R1}', n_{I1}'). These eight unknown parameters can be obtained by solving the above eight independent equations. The equilibrium mole fractions of compound R at a given T, x_R (in liquid-phase L) and x_R' (in liquid-phase L′), are given by

$$x_R = \frac{n_{R0}}{n_{R0} + n_{I0}} \tag{9}$$

$$x_R' = \frac{n_{R0}'}{n_{R0}' + n_{I0}'} \tag{10}$$

The solutions of the above eight coupled equations are easily obtained analytically. From eqs 3 and 5, we have

$$n_{R1} = n_{R0}\frac{v_1}{v_0} \tag{11}$$

Similarly eqs 4 and 6 give

$$n_{R1}' = n_{R0}'\frac{v_1'}{v_0'} \tag{12}$$

By inserting eqs 11 and 12 into eq 8 and using eq 7, n_{R0} and n_{R0}' can be solved as

$$n_{R0} = \frac{n_{RT1} - n_{g1} - (v_1'/v_0')(n_{RT0} - n_{g0})}{v_1/v_0 - v_1'/v_0'} \tag{13}$$

$$n_{R0}' = \frac{n_{RT1} - n_{g1} - (v_1/v_0)(n_{RT0} - n_{g0})}{v_1'/v_0' - v_1/v_0} \tag{14}$$

Then, n_{R1} and n_{R1}' can be obtained from eqs 11 and 12.

Concerning the compound I liquid moles, we have the following relations from eqs 5 and 6:

$$n_{I0} = n_{I1}\frac{n_{R0}}{n_{R1}} \tag{15}$$

$$n_{I0}' = n_{I1}'\frac{n_{R0}'}{n_{R1}'} \tag{16}$$

By inserting eqs 15 and 16 into eqs 1 and 2, n_{I1} and n_{I1}' can be solved using eqs 11 and 12:

$$n_{I1} = \frac{n_{IT0} - n_{IT1}(v_0'/v_1')}{v_0/v_1 - v_0'/v_1'} \tag{17}$$

$$n_{I1}' = \frac{n_{IT0} - n_{IT1}(v_0/v_1)}{v_0'/v_1' - v_0/v_1} \tag{18}$$

Then, n_{I0} and n_{I0}' can be obtained by eqs 15 and 16. Thus, mole fractions (eqs 9 and 10) and molar volumes (eqs 3 and 4) for each liquid can be determined.

Materials. Ionic liquid [bmim][PF_6] (Lot and Filling Nos. 1152140 and 50705138, assay ≥ 96.0 %, Chemical Abstracts Service Registry No. (CASRN) 174501-64-5) was obtained from Fluka Chemika (Buchs, Switzerland). The as-received water mass fraction was 0.23 % and was measured by Karl Fischer titration (Aqua-Star C3000 and Aqua-Star Coulomat C and A solutions). The as-received chlorine content was measured using two methods. The extractable chlorine content was 4.7 mg·cm^{-3} and was measured by ion chromatography (Dionex AS17 column). The bound chlorine content was 0.79 ppm by mass and was measured using a Wickbold torch method. The [bmim][PF_6] was dried by heating and stirring in a Pyrex glass tube to 348.15 K (PolyScience constant-temperature bath, model 1157) while under a vacuum of 5×10^{-4} Pa (Pfeiffer turbo vacuum pump, model TSH 071) for a minimum of 10 days to remove any trace amounts of water or other impurities. The final water mass fraction after drying was 0.0186 %.

1,1,1,2-Tetrafluoroethane (R-134a, CASRN 811-97-2), 1,1,1-trifluoroethane (R-143a, CASRN 420-46-2), and 1,1-difluoroethane (R-152a, CASRN 75-37-6) were obtained from DuPont Fluoroproducts (Wilmington, DE). R-134a and R-152a had a minimum mole fraction purity of 99.9 %, and R-143a had a mole fraction purity of 99.0 %.

Fluoromethane (R-41, CASRN 593-53-3) and fluoroethane (R-161, CASRN 353-36-6) were obtained from Speciality Gases of America (Toledo, OH) with a minimum mole fraction purity of 99 % (major impurity chloromethane) and 97 % (major impurity unsaturates), respectively. The purity of the gases were determined using a gas chromatography method (Agilent 6890N, Restek Rtx-200 column, 105 m × 0.25 mm).

Experimental Method. High-pressure sample containers were fabricated from borosilicate glass tubing with an outside diameter of 6.41 mm, an inside diameter of 3.94 mm, and an overall length of 10 cm. The glass tubing was sealed at one end and open at the other. The borosilicate glass tubes were cleaned before using in an ultrasonic bath filled with acetone for 2 h and dried overnight in a vacuum oven at 348.15 K. The borosilicate glass tubing was chosen for three reasons: (i) zero fluorocarbon permeability, (ii) visual clarity for easily measuring heights of the liquid phases, and (iii) good pressure and temperature rating. The high-pressure glass tubing had a wall thickness of 1.235 mm with a pressure rating of 4.7 MPa at 298.15 K. A protective shell made from clear polycarbonate was machined to encapsulate the glass tube as shown in Figure 1. One end of the plastic shell was sealed, and the other end was threaded such that a Swagelok fitting (model SS-2-TA-1-OR) and ball valve (model SS-41GS2) could be attached and sealed using a Teflon O-ring between the open end of the glass tubing and the face of the fitting. The open ball valve allowed a syringe needle to be inserted into the tubing for the addition of the ionic liquid, but yet could be closed after the tube was evacuated to prevent air from reentering. The entire assembly was hydrostatically pressure tested to 7.7 MPa, and no leaks were observed. The Swagelok ball valve was chosen due to its excellent pressure and temperature rating of 17.3 MPa and 422 K and its compatibility with hydrofluorocarbon refrigerant gases. The volume of each liquid layer was obtained by measuring the liquid height from the bottom of the glass tubing, as illustrated in Figure 1, using an electronic caliper (Mitutoyo Corp., model no. CD-6″ CS, code no. 500-196) with an accuracy of ± 0.01 mm. The volume, v, versus the height, h, was calibrated experimentally, and an excellent linear relation, $v = a + bh$, was obtained. The a and b parameters were obtained

Table 1. Experimental VLLE Results for R-41 (R) + [bmim][PF_6] (I) System[a]

T/K	100 x_R'	100 x_R	V'/cm^3·mol^{-1}	V/cm^3·mol^{-1}	$V^{E'}$/cm^3·mol^{-1}	V^{E}/cm^3·mol^{-1}
243.2	81.8 ± 1.0	100.0 ± 1.0	67.6 ± 1.0	43.8 ± 1.0	−5.3 ± 1.0	−0.6 ± 1.0
263.2	80.7 ± 1.0	99.9 ± 1.0	71.2 ± 1.0	47.8 ± 1.0	−6.8 ± 1.0	−0.3 ± 1.0
294.1	74.6 ± 1.0	100.0 ± 0.3	82.7 ± 1.0	55.9 ± 1.0	−12.6 ± 1.0	−1.4 ± 1.0

[a] x_R', mole fraction in lower liquid phase; x_R, mole fraction in upper liquid phase; V', molar volume in lower liquid phase; V, molar volume in upper liquid phase; $V^{E'}$, excess molar volume in lower liquid phase; V^{E}, excess molar volume in upper liquid phase.

Table 2. Experimental VLLE Results for R-134a (R) + [bmim][PF_6] (I) System[a]

T/K	100 x_R'	100 x_R	V'/cm^3·mol^{-1}	V/cm^3·mol^{-1}	$V^{E'}$/cm^3·mol^{-1}	V^{E}/cm^3·mol^{-1}
318.2	69.5 ± 2.0	101.2 ± 1.5	114.7 ± 5.0	88.5 ± 5.0	−12.4 ± 5.0	−2.1 ± 5.0
333.8	63.8 ± 2.0	99.4 ± 0.3	127.4 ± 3.0	96.6 ± 1.5	−11.4 ± 3.0	−1.3 ± 1.5
355.0	57.5 ± 2.0	99.1 ± 1.0	139.0 ± 5.0	110.7 ± 5.0	−16.7 ± 5.0	−1.9 ± 5.0

[a] x_R', mole fraction in lower liquid phase; x_R, mole fraction in upper liquid phase; V', molar volume in lower liquid phase; V, molar volume in upper liquid phase; $V^{E'}$, excess molar volume in lower liquid phase; V^{E}, excess molar volume in upper liquid phase.

for each tube using methyl alcohol as a calibration fluid at 293.15 K.

The sample containers were initially evacuated and weighed to determine the tare mass. The samples were then prepared in a nitrogen purged drybox to minimize water contact with the hygroscopic [bmim][PF_6]. A syringe was used to add the required amount of [bmim][PF_6] through the open ball valve, and the sample was weighed to determine the mass of [bmim][PF_6] added. With the ball valve closed, the sample container was removed from the drybox. A vacuum pump (Edwards, model E2M1.5) was used to evacuate the nitrogen from inside the sample container. A heat gun (Master Appliance Corporation, model HG-201A) was used to carefully heat the sample to assist with the removal of any nitrogen that may have dissolved in the ionic liquid while open in the drybox. The sample valve was then connected to the appropriate refrigerant cylinder. The refrigerant cylinders were inverted in order to dispense liquid refrigerant into the sample container. The sample container was cooled in dry ice for approximately 5 min prior to filling with liquid refrigerant. Caution was taken not to completely fill the sample container with liquid refrigerant. If the sample container was overfilled with liquid refrigerant such that no vapor volume could be viewed, the ball valve was slowly opened to vent the liquid refrigerant to a safe level. The thermal expansion of the liquid refrigerant during warming could cause the pressure to rapidly increase if the sample container was completely filled with liquid refrigerant and could exceed the pressure rating of the glass tubing. Once filled with refrigerant, the sample containers were reweighed to determine the mass of liquid refrigerant added and then shaken to begin the mixing process. The sample container masses were checked after several days to ensure that no refrigerant was leaking. The masses remained constant within the accuracy (± 0.0001 g) of the balance (Mettler Toledo, model AG204) even after several weeks. If a small amount of refrigerant does leak out, reweighing the sample container and adjusting for the lost moles of refrigerant (assuming negligible amount of [bmim][PF_6] escaped in vapor phase) corrected for this error.

To establish the thermodynamic equilibrium, sufficient time and mixing are required. A custom-made mixing apparatus, which can hold 14 high-pressure sample containers, was designed for rocking the tubes back and forth in a constant-temperature bath (Tamson Instruments, TV4000LT) with a viewing window. Additional details about the mixing apparatus can be found in ref 3. The bath was filled with Dow Corning silicon oil (type 5010) with a recommended use range of (233.15 < T < 403.15) K. The bath had excellent temperature control with a uniformity of ± 0.2 K, and a NIST traceable RTD (Hart Scientific, model 1560) was used to verify the accuracy of the temperature measurement. Before height measurements were taken, the sample holder was positioned upright below the liquid level of the tank for (6 to 12) h. The volume of each liquid layer was obtained by measuring the liquid height from the bottom of the glass tube as illustrated in Figure 1 using the electronic caliper. The uncertainty in the mole fraction is estimated to be ± 0.01 %. The uncertainty in the volume is estimated to be ± 0.25 %.

Results

Measurement Results. The most difficult problem of the experiments was to establish the equilibrium state. By monitoring the change in the height of each phase until no further change occurred, it was assured that equilibrium had been reached. Mixing time to reach equilibrium can take several days and is one of the most critical properties for properly measuring VLLE whether using this method or the more common cloud-point method.[8−16] The time required to effectively mix the ionic liquid and refrigerant and reach equilibrium is also a function of the fluid viscosity (i.e., temperature) and decreases at higher temperature (i.e., viscosity decreases).

To account for a change in the interior volume of the tubes at high temperature, the thermal expansion coefficient for borosilicate glass ($\alpha = 3.3 \times 10^{-6}$/K)[18] was used for uncertainty estimation. The linear expansion can be ignored and the area expansion results in a change in the overall height measurement of 0.05 mm (initial height 100 mm). This small change in the height measurement leads to a minimal change in the mole fractions, $\Delta x_R'$ and Δx_R, of 1×10^{-3} % and molar volumes, $\Delta V'$ and ΔV, of 0.02 cm^3·mol^{-1} (i.e., 2-butanol + water)[3].

Total uncertainties in the final composition and molar volume determination are provided in Tables 1 to 7. Total uncertainties ($\delta x_{TE} = \sqrt{\delta x_{RE}^2 + \delta x_{SE}^2}$) were estimated by calculating both the overall random (δx_{RE}) and systematic uncertainty (δx_{SE}). The overall random uncertainties were estimated using the following uncertainty propagation method:

$$\delta x_{RE} = \sqrt{\sum_{i=1}^{n}\left[\delta p_i\left(\frac{\partial x}{\partial p_i}\right)\right]^2} \qquad (19)$$

where δx_{RE} is the mole fraction or molar volume random uncertainty of the liquid composition, $\partial x/\partial p_i$ is the partial derivative of x with respect to the ith experimental parameter p_i, which is calculated from the sensitivity analysis of each

Table 3. Experimental VLLE Results for R-143a (R) + [bmim][PF_6] (I) System[a]

T/K	100 x_R'	100 x_R	V'/cm^3·mol^{-1}	V/cm^3·mol^{-1}	$V^{E'}$/cm^3·mol^{-1}	V^{E}/cm^3·mol^{-1}
291.8	29.0 ± 1.0	100.7 ± 1.0	163.1 ± 1.0	89.2 ± 1.0	−9.2 ± 1.0	1.3 ± 1.0
324.6	25.8 ± 1.0	100.1 ± 1.0	178.8 ± 1.0	105.6 ± 1.0	−5.2 ± 1.0	−0.3 ± 1.0
338.6	24.0 ± 1.0	100.7 ± 1.0	181.3 ± 1.0	124.1 ± 1.0	−10.5 ± 1.0	−0.7 ± 1.0

[a] x_R', mole fraction in lower liquid phase; x_R, mole fraction in upper liquid phase; V', molar volume in lower liquid phase; V, molar volume in upper liquid phase; $V^{E'}$, excess molar volume in lower liquid phase; V^{E}, excess molar volume in upper liquid phase.

Table 4. Experimental VLLE Results for R-152a (R) + [bmim][PF_6] (I) System[a]

T/K	100 x_R'	100 x_R	V'/cm^3·mol^{-1}	V/cm^3·mol^{-1}	$V^{E'}$/cm^3·mol^{-1}	V^{E}/cm^3·mol^{-1}
318.3	77.4 ± 1.0	96.1 ± 1.0	80.5 ± 5.0	78.0 ± 5.0	−27.5 ± 5.0	−5.2 ± 5.0
333.8	72.2 ± 1.0	95.0 ± 1.0	93.2 ± 3.0	76.6 ± 5.0	−25.6 ± 3.0	−12.7 ± 5.0
354.9	67.6 ± 1.0	98.7 ± 1.0	118.2 ± 5.0	78.6 ± 5.0	−13.7 ± 5.0	−15.1 ± 5.0

[a] x_R', mole fraction in lower liquid phase; x_R, mole fraction in upper liquid phase; V', molar volume in lower liquid phase; V, molar volume in upper liquid phase; $V^{E'}$, excess molar volume in lower liquid phase; V^{E}, excess molar volume in upper liquid phase.

Table 5. Experimental VLLE Results for R-161 (R) + [bmim][PF_6] (I) System[a]

T/K	100 x_R'	100 x_R	V'/cm^3·mol^{-1}	V/cm^3·mol^{-1}	$V^{E'}$/cm^3·mol^{-1}	V^{E}/cm^3·mol^{-1}
243.2	76.1 ± 2.0	102.1 ± 2.5	72.3 ± 3.0	49.7 ± 2.0	−21.4 ± 3.0	−10.4 ± 2.5
263.2	71.8 ± 1.0	102.0 ± 2.0	78.0 ± 1.0	52.6 ± 1.0	−24.5 ± 1.0	−10.3 ± 2.0
293.7	68.9 ± 1.0	100.2 ± 0.3	83.1 ± 1.0	59.7 ± 1.0	−28.4 ± 1.0	−8.5 ± 1.0
324.6	62.5 ± 1.0	100.0 ± 2.0	104.6 ± 5.0	73.6 ± 5.0	−22.3 ± 5.0	−2.3 ± 5.0
338.6	60.8 ± 1.0	100.8 ± 2.0	120.4 ± 15.0	81.7 ± 5.0	−12.5 ± 15.0	0.5 ± 10.0

[a] x_R', mole fraction in lower liquid phase; x_R, mole fraction in upper liquid phase; V', molar volume in lower liquid phase; V, molar volume in upper liquid phase; $V^{E'}$, excess molar volume in lower liquid phase; V^{E}, excess molar volume in upper liquid phase.

Table 6. Experimental VLLE Results for R-23 (R) + [bmim][PF_6] (I) System[2] [a]

T/K	100 x_R'	100 x_R	V'/cm^3·mol^{-1}	V/cm^3·mol^{-1}	$V^{E'}$/cm^3·mol^{-1}	V^{E}/cm^3·mol^{-1}
280.2	85.3 ± 2.0	99.6 ± 0.3	79.4 ± 3.0	70.6 ± 3.0	−12.0 ± 3.0	−1.7 ± 3.0
285.6	81.2 ± 2.0	99.7 ± 0.3	86.5 ± 3.0	73.6 ± 3.0	−14.0 ± 3.0	−2.8 ± 3.0
293.6	77.3 ± 2.0	100.1 ± 0.3	87.8 ± 3.0	86.2 ± 3.0	−26.2 ± 3.0	−0.2 ± 3.0

[a] x_R', mole fraction in lower liquid phase; x_R, mole fraction in upper liquid phase; V', molar volume in lower liquid phase; V, molar volume in upper liquid phase; $V^{E'}$, excess molar volume in lower liquid phase; V^{E}, excess molar volume in upper liquid phase.

Table 7. Experimental VLLE Results for R-125 (R) + [bmim][PF_6] (I) System[3] [a]

T/K	100 x_R'	100 x_R	V'/cm^3·mol^{-1}	V/cm^3·mol^{-1}	$V^{E'}$/cm^3·mol^{-1}	V^{E}/cm^3·mol^{-1}
285.8	69.5 ± 2.0	99.1 ± 0.2	118.9 ± 2.5	96.0 ± 0.5	−10.3 ± 2.5	−0.4 ± 0.5
294.8	61.8 ± 2.0	99.5 ± 0.2	129.2 ± 2.5	100.1 ± 0.5	−11.0 ± 2.5	−0.2 ± 0.5
313.1	48.3 ± 2.0	99.7 ± 0.2	147.5 ± 2.5	110.5 ± 0.5	−14.1 ± 2.5	0 ± 0.5

[a] x_R', mole fraction in lower liquid phase; x_R, mole fraction in upper liquid phase; V', molar volume in lower liquid phase; V, molar volume in upper liquid phase; $V^{E'}$, excess molar volume in lower liquid phase; V^{E}, excess molar volume in upper liquid phase.

parameter, and δp_i is the estimated uncertainty of the experimental parameter p_i. The following 12 experimental parameters were considered to have an effect on the random uncertainties: a, b, n_{g0}, n_{g1}, h', and h for both sample containers (sample 0 and sample 1). The heights were found to have the largest overall effect on the random uncertainties. The systematic uncertainties (δx_{SE}) include properly correcting for the area expansion, meniscus, and vapor phase moles.

The uncertainty estimation for neglecting the vapor moles was calculated for R-134a + [bmim][PF_6] at T = 355.0 K. Assuming the vapor was composed of pure R-134a (i.e., [bmim][PF_6] has negligible vapor pressure), the vapor moles resulted in a change in the mole fractions ($\Delta x_R'$ = 6.1 % and Δx_R = 0.02 %) and molar volumes ($\Delta V'$= 20.0 cm^3·mol^{-1} and ΔV= 1.1 cm^3·mol^{-1}). In the case of high-pressure refrigerant gases, the moles of vapor were not neglected.

The present experimental results (mole fraction, molar volume, and excess molar volume) for each liquid phase of the binary systems (R-41 + [bmim][PF_6], R-134a + [bmim][PF_6], R-143a + [bmim][PF_6], R-152a + [bmim][PF_6], and R-161 + [bmim][PF_6]) are summarized in Tables 1 to 5, respectively. In addition, the previous reported results for R-23 + [bmim][PF_6][2] and R-125 + [bmim][PF_6][3] are also provided in Tables 6 and 7, respectively, for the purpose of comparison.

To prove the existence of a LCST of the VLLE curve, cloud-point measurements have also been made. Three samples of [bmim][PF_6] containing both R-134a and R-152a were prepared. Starting at a low temperature of 293.15 K, where only one liquid phase existed, the temperature was slowly raised (1 K·h^{-1}) until a second liquid phase began to appear. The observed cloud-point mole fractions for R-134a were 74.1 % at (312.3 ± 2) K, 79.4 % at (305.5 ± 2) K, and 85.1 % at (302.2 ± 2) K. The observed cloud-point mole fractions for R-152a were 73.3 % at (327.8 ± 2) K, 78.9 % at (315.6 ± 2) K, and 85.2 % at (303.4 ± 2) K. Based on these measurements, the LCST for R-134a is estimated to be about 296 K at about a mole fraction of 88 % of R-134a and the LCST for R-152a is estimated to be about 302 K at about a mole fraction of 88 % of R-152a.

Model Comparisons of VLLE Results. In this report, we have employed a Redlich−Kwong EOS[1,2,4] to predict VLLE behavior of HFCs in RTILs. EOS model structure and parameters are provided in the Supporting Information. The EOS model predictions have been compared with observed VLE and VLLE

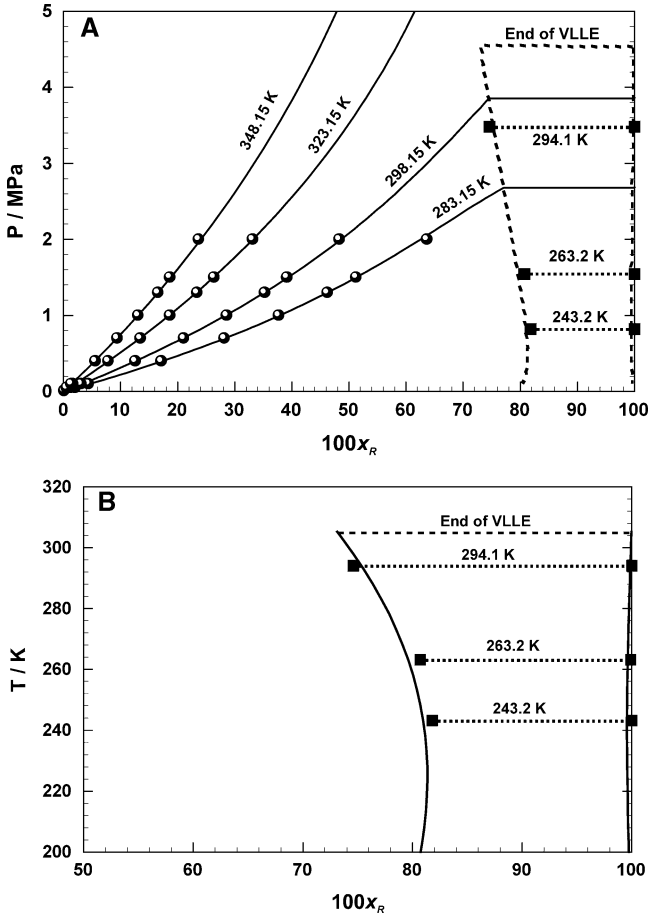

Figure 2. (A) Pressure−composition and (B) temperature−composition phase diagram for R-41 (R) (fluoromethane) + [bmim][PF_6] (I) (1-butyl-3-methylimidazolium hexafluorophosphate). Solid and dashed lines predicted by our EOS. Symbols: ●, VLE data;[22] ■, the present VLLE data.

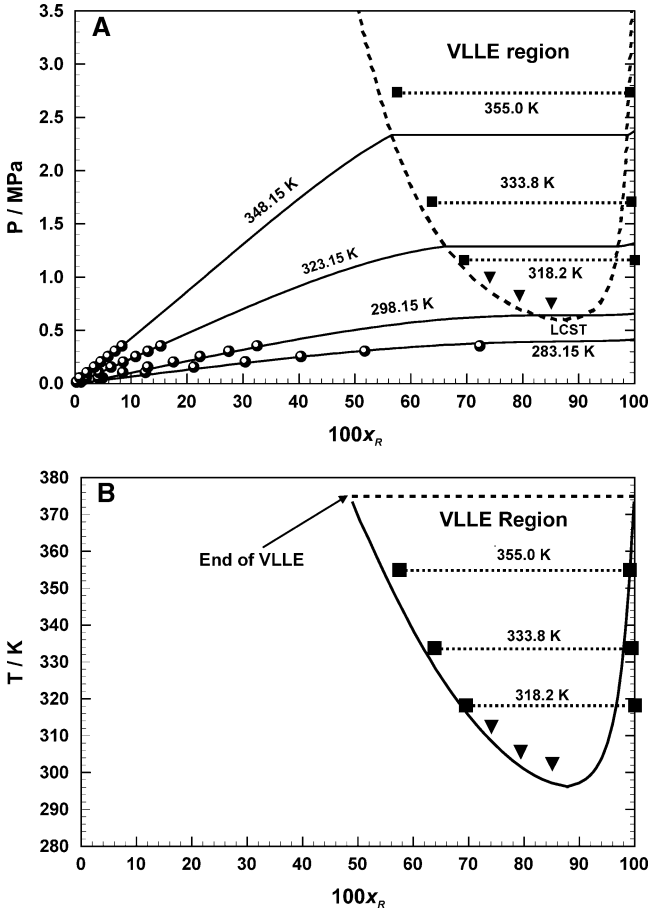

Figure 3. (A) Pressure−composition and (B) temperature−composition phase diagram for R-134a (R) (1,1,1,2-tetrafluoroethane) + [bmim][PF_6] (I) (1-butyl-3-methylimidazolium hexafluorophosphate). Solid and dashed lines predicted by our EOS. Symbols: ●, VLE data;[5] ■, the present VLLE data; ▼, the present cloud-point data.

data for each binary pair in Figures 2 to 6 using isothermal *Px* (pressure−composition) and *Tx* (temperature−composition) phase diagrams. In all cases there is reasonable agreement with the experimental VLLE data. In particular, by considering the fact that only VLE data have been used to develop the EOS model, it may be fair to say that the present agreement of VLLE data with the model is even extraordinary.

Discussion

Using only VLE data, the present EOS model has predicted the VLLE phase behavior for HFCs in RTILs. In the case of R-134a and R-152a shown in Figures 3 and 5, the VLLE measurements confirm the type-V mixture behavior according to the classification of van Konynenburg and Scott,[19,20] and the EOS model is in good agreement with the measurements. The cloud-point measurements are plotted on the same figures to show the existence of the LCST and provide further confirmation that these binary systems belong to the type-V mixture behavior. In this respect, it should be mentioned here that the present EOS model predicts another VLLE curve in very low temperatures with upper critical solution temperatures (UCST) of about 200 K at a mole fraction of 90 % for R-134a and 203 K at mole fraction of 77 % for R-152a. This indicates type-IV behavior. However, such VLLE phases most likely interfere with solid phases as discussed in refs 2 and 3: crystallization (236.15 K) and glass transition (197.15 K) for [bmim][PF_6],[21] and triple point (169.9 K)[17] for R-134a and triple point (154.6 K)[17] for R-152a. Thus, the present systems will be characterized as type-V mixture behavior. In the case of R-143a and R-161 shown in Figures 4 and 6, LCST occurs at the very low temperatures, where solid phases will interfere. As for R-41 shown in Figure 2, no LCST exists. Therefore, it suggests these binary systems belong to type-III mixture behavior.[19,20]

Our previous measured VLE for difluoromethane (R-32)[5,6] and 1,1,2,2-tetrafluoroethane (R-134)[22] show that these compounds have particularly high solubility in [bmim][PF_6], and our EOS model does not predict VLLE behavior below the critical temperature of these refrigerants (T_c for R-32 is 351.3 K[17] and T_c for R-134 is 392.2 K[22]). VLLE might exist above the critical temperature, which would classify these binary systems as type-V mixture behavior, but if no VLLE exists, then these systems will be the simple type-I mixture behavior.

One of the most useful information in the present method is to be able to obtain the molar volume of each separated liquid simultaneously with the mole fraction of each liquid at any given isothermal condition. Then, the excess molar volume of each liquid solution ($V^{E'}$ and V^E) can be obtained, by use of the pure component molar volumes (V_R^0 and V_I^0 for compounds R and I) using:

$$V^{E'} = V_m - x_R' V_R^0 - x_I' V_I^0 \text{ or } V^E = V_m - x_R V_R^0 - x_I V_I^0 \quad (20)$$

where V_m is the measured molar volume of the mixture ($V_m = V'$ for phase L′ or $V_m = V$ for phase L), and (x_R', x_I' or x_R, x_I) are mole fractions of compound R and compound I in phase L′

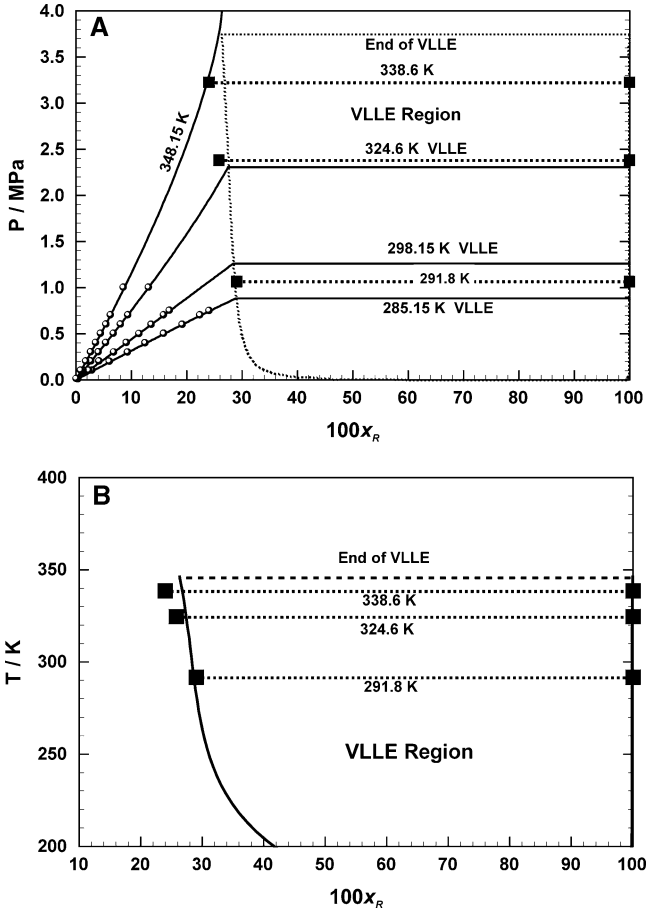

Figure 4. (A) Pressure−composition and (B) temperature−composition phase diagram for R-143a (R) (1,1,1-trifluoroethane) + [bmim][PF_6] (I) (1-butyl-3-methylimidazolium hexafluorophosphate). Solid and dashed lines predicted by our EOS. Symbols: ●, VLE data;[5] ■, the present VLLE data.

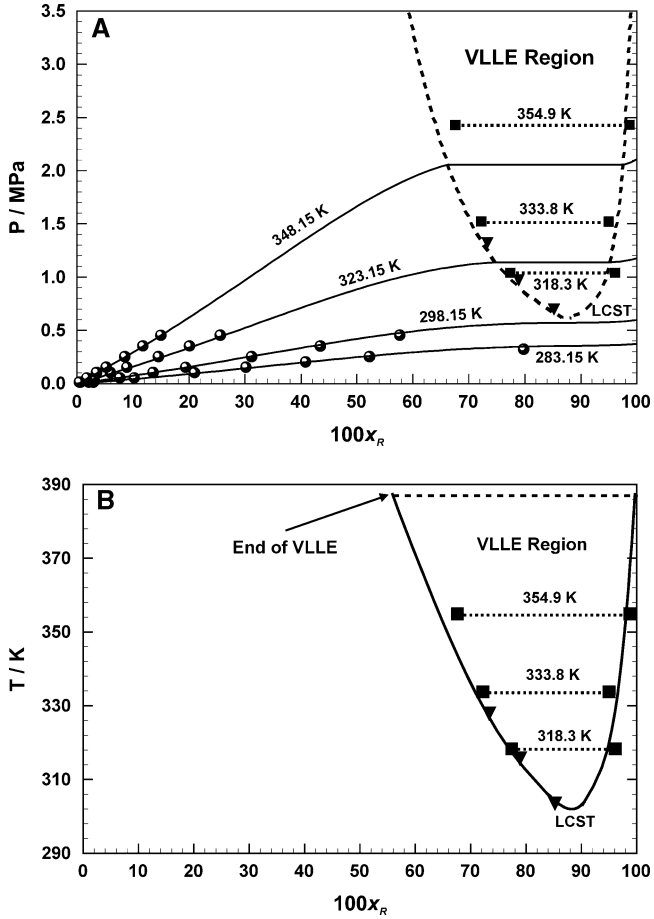

Figure 5. (A) Pressure−composition and (B) temperature−composition phase diagram for R-152a (R) (1,1-difluoroethane) + [bmim][PF_6] (I) (1-butyl-3-methylimidazolium hexafluorophosphate). Solid and dashed lines predicted by our EOS. Symbols: ●, VLE data;[5] ■, the present VLLE data; ▼, the present cloud-point data.

and L, respectively. Saturated liquid molar volumes of refrigerants were calculated with the EOS computer program.[17] Observed large negative excess molar volumes in [bmim][PF_6]-rich side liquids are noteworthy as shown in Tables 1 to 7. The magnitude of $V^{E'}$ is more than 10 times larger than that of ordinary liquid mixtures (typically about (0 ± 3) $cm^3 \cdot mol^{-1}$).[23−29] The largest negative excess molar volumes reported in the literature are for a system with strong intermolecular interactions (acetic acid + triethylamine) at $T = 298$ K with an excess molar volume of about -12 $cm^3 \cdot mol^{-1}$.[23,30] Concerning $V^{E'}$, it should be mentioned that similarly large negative excess volumes have been reported for R-23, R-125, and CO_2 mixtures with ionic liquid [bmim][PF_6].[2,3]

Mixtures of ionic liquid [bmim][PF_6] with gases such as HFCs and CO_2 have quite large negative excess molar volumes as compared with what have been reported with ordinary mixtures.[23] This is a unique and new finding; yet it is not surprising as discussed in our previous papers.[2,3] Still the large negative excess molar volumes pose an interesting challenge for theoretical modelers to explain this phenomena. One possible explanation for CO_2 + [bmim][PF_6] system using molecular dynamic calculations by Huang et al.[31] indicates that small angular rearrangements of the anion are occurring which create localized cavities that allow CO_2 to fit above and below the imidazolium ring without much change from the molar volume of pure [bmim][PF_6]. Although it is not quite clear yet, an additional force such as hydrogen bonding may also be involved with mixtures of HFCs and [bmim][PF_6].

On the other hand, the HFC-rich side liquids except for R-152a are practically 100 mol % refrigerant (within experimental error); therefore, in these cases the excess molar volume, V^E, should be zero. In the case of R-152a, the HFC-rich liquid-phase L contains a mole fraction of about (1 to 5) % [bmim]-[PF_6], and the excess volume as expected is negative. Tables 1 to 7 show that V^E is zero (within experimental error), except for R-152a mentioned above and R-161. The excess molar volume for R-161-rich side liquids are expected to be zero because the liquid is essentially 100 mol % refrigerant, while experimental values are large negative below 293.7 K in Table 5. One explanation for this discrepancy is that the thermophysical properties for R-161 are not well-defined yet in the literature,[32] and another reason is that our sample had a mole fraction purity of only 97 %, as mentioned earlier. Analytical analysis of the R-161 indicates that the refrigerant contains a mixture of unidentified olefins, and so the R-161 + [bmim]-[PF_6] mixture cannot be regarded as a binary mixture due to the impurity content. The present method based on the Gibbs phase rule is only applicable for a binary system. Thus, rather large uncertainties and inconsistent excess molar volumes in Table 5 are likely due to the large impurity content (i.e., nonbinary system).

Conclusions

A simple experimental method to characterize VLLE has been developed based only on mass-and-volume measurements. The global phase behavior of the binary systems (R-134a + [bmim]-

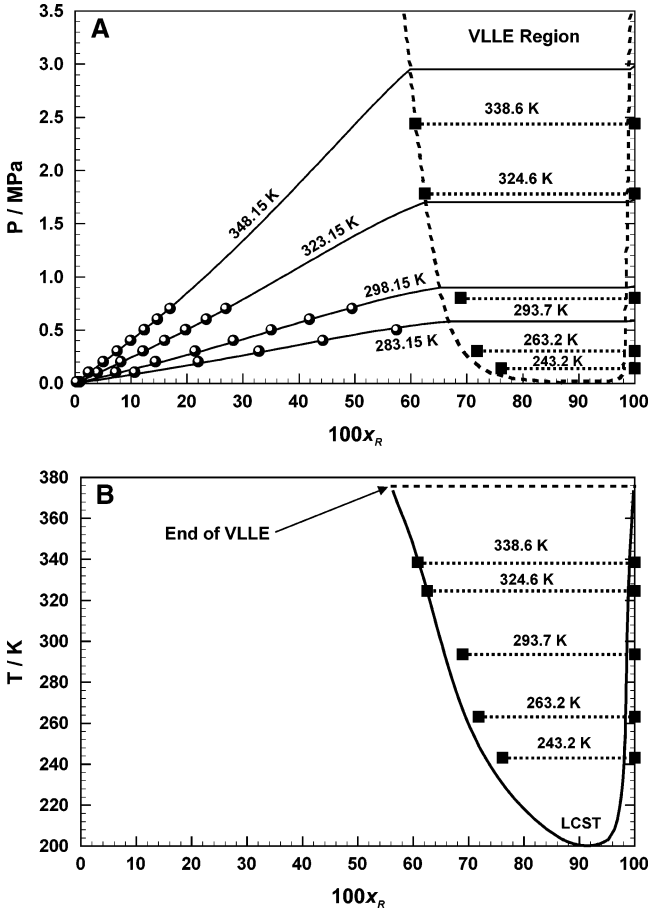

Figure 6. (A) Pressure−composition and (B) temperature−composition phase diagram for R-161 (R) (fluoroethane) + [bmim][PF_6] (I) (1-butyl-3-methylimidazolium hexafluorophosphate). Solid and dashed lines predicted by our EOS. Symbols: ●, VLE data;[22] ■, the present VLLE data.

[PF_6] and R-152a + [bmim][PF_6]) has been confirmed as type-V, based on our EOS model, which has been validated by the present VLLE and cloud-point data. The binary systems (R-41 + [bmim][PF_6], R-143a + [bmim][PF_6], and R-161 + [bmim]-[PF_6]) belong to the type-III phase behavior. Also, the present study shows that our EOS model based on low-pressure VLE data alone can be highly reliable when extrapolating thermodynamic properties. Finally, large negative excess molar volumes in the present systems have been measured.

Acknowledgment

The authors thank Mr. Joseph Nestlerode for the vapor−liquid−liquid equilibria measurements.

Supporting Information Available:

EOS model structure and parameters. This material is available free of charge via the Internet at http://pubs.acs.org.

Literature Cited

(1) Shiflett, M. B.; Yokozeki, A. Solubilities and diffusivities of carbon dioxide in ionic liquids: [bmim][PF_6] and [bmim][BF_4]. *Ind. Eng. Chem. Res*. **2005**, *44*, 4453−4464.

(2) Yokozeki, A.; Shiflett, M. B. Global phase behaviors of trifluoromethane in room-temperature ionic liquid [bmim][PF_6]. *AIChE J*. (submitted for publication).

(3) Shiflett, M. B.; Yokozeki, A. Vapor−liquid−liquid equilibria of pentafluoroethane and ionic liquid [bmim][PF_6] mixtures studied with the volumetric method. *J. Phys. Chem. B* (in press).

(4) Yokozeki, A.; Shiflett, M. B. Thermodynamic phase behaviors of carbon dioxide and hydrofluorocarbons in ionic liquids. *Proceedings of the 1st International Congress on Ionic Liquids*, Salzburg, Austria, June 19−22, 2005; p 112.

(5) Shiflett, M. B.; Yokozeki, A. Solubility and diffusivity of hydrofluorocarbons in room-temperature ionic liquids. *AIChE J*. **2006**, *52*, 1205−1219.

(6) Shiflett, M. B.; Harmer, M. A.; Junk, C. P.; Yokozeki, A. Solubility and diffusivity of difluoromethane in room-temperature ionic liquids. *J. Chem. Eng. Data* **2006**, *51*, 483−495.

(7) Shiflett, M. B.; Harmer, M. A.; Junk, C. P.; Yokozeki, A. Solubility and diffusivity of 1,1,1,2-tetrafluoroethane in room-temperature ionic liquids. *Fluid Phase Equilib*. **2006**, *242*, 220−232.

(8) Ochi, K.; Saito, T.; Kojima, K. Measurement and correlation of mutual solubilities in 2-butanol + water. *J. Chem. Eng. Data* **1996**, *41*, 361−364.

(9) Hefter, G. T.; Barton, A. F. M.; Chand, A. Semiautomated apparatus for the determination of liquid solubilities: mutual solubilities of water and butan-2-ol. *J. Chem. Soc., Faraday Trans*. **1991**, *87*, 591−596.

(10) Moriyoshi, T.; Kaneshina, S.; Aihara, K.; Yabumoto, K. Mutual solubility of 2-butanol + water under high pressure. *J. Chem. Thermodyn*. **1975**, *7*, 537−545.

(11) Wu, C.-T.; Marsh, K. N.; Deev, A. V.; Boxall, J. A. Liquid−liquid equilibria of room-temperature ionic liquids and butan-1-ol. *J. Chem. Eng. Data* **2003**, *48*, 486-491.

(12) Heintz, A.; Lehmann, J. K.; Wertz, C. Thermodynamic properties of mixtures containing ionic liquids. 3. Liquid−liquid equilibria of binary mixtures of 1-ethyl-3-methylimidazolium bis(trifluoromethylsulfonyl)-imide with propan-1-ol, butan-1-ol, and pentan-1-ol. *J. Chem. Eng. Data* **2003**, *48*, 472−474.

(13) Crosthwaite, J. M.; Aki, S. N. V. K.; Maginn, E. J.; Brennecke, J. F. Liquid-phase behavior of imidazolium-based ionic liquids with alcohols. *J. Phys. Chem. B* **2004**, *108*, 5113−5119.

(14) Crosthwaite, J. M.; Aki, S. N. V. K.; Maginn, E. J.; Brennecke, J. F. Liquid-phase behavior of imidazolium-based ionic liquids with alcohols: effect of hydrogen bonding and non-polar interactions. *Fluid Phase Equilib*. **2005**, *228−229*, 303−309.

(15) Wagner, M.; Stanga, O.; Schröer, W. The liquid−liquid coexistence of binary mixtures of the room-temperature ionic liquid 1-methyl-3-hexylimidazolium tetrafluoroborate with alcohols. *Phys. Chem. Chem. Phys*. **2004**, *6*, 4421−4431.

(16) Wagner, M.; Stanga, O.; Schröer, W. Corresponding states analysis of the critical points in binary solutions of room-temperature ionic liquids. *Phys. Chem. Chem. Phys*. **2003**, *5*, 3943−3950.

(17) Lemmon, E. W.; McLinden, M. O.; Huber, M. L. NIST reference fluid thermodynamic and transport properties. *REFPROP*, *Version 7.0, Users' Guide*; U.S. Department of Commerce, Technology Administration, National Institute of Standards and Technology, Standard Reference Data Program: Gaithersburg, MD, 2002.

(18) Perry, R. H.; Green, D. W. *Perry's Chemical Engineers' Handbook*, 7th ed.; McGraw-Hill: New York, 1997; pp 10−126.

(19) Scott, R. L.; van Konynenburg, P. H. Static properties of solutions. van der Waals and related models for hydrocarbon mixtures. *Discuss. Faraday Soc*. **1970**, *49*, 87−97.

(20) Van Konynenburg, P. H.; Scott, R. L. Critical lines and phase equilibria in binary van der Waals mixtures. *Philos. Trans. R. Soc. A* **1980**, *298*, 495−540.

(21) Fredlake, C. P.; Crosthwaite, J. M.; Hert, D. G.; Aki, S. N. V. K.; Brennecke, J. F. Thermophysical properties of imidazolium-based ionic liquids. *J. Chem. Eng. Data* **2004**, *49*, 954−964.

(22) Shiflett, M. B.; Yokozeki, A. Gaseous absorption of fluoromethane, fluoroethane, and 1,1,2,2-tetrafluoroethane in 1-butyl-3-methylimidazolium hexafluorophosphate. *Ind. Chem. Eng. Res.* (in press).

(23) Rowlinson, J. S.; Swinton, F. L. *Liquids and Liquid Mixtures*; Butterworth: London, 1982.

(24) Hoheisel, C.; Deiters, U.; Lucas, K. The extension of pure fluid thermodynamic properties to supercritical mixtures−a comparison of current theories with computer data over a large region of states. *Mol. Phys*. **1983**, *49*, 159−170.

(25) Singer, V. L.; Singer, K. Monte Carlo calculation of thermodynamic properties of binary mixtures of Lennard−Jones (12−6) liquids. *Mol. Phys*. **1972**, *24*, 357−390.

(26) Grenner, A.; Klauck, M.; Kramer, M.; Schmelzer, J. Activity coefficients at infinite dilution of cyclohexylamine + octane, toluene, ethylbenzene, or aniline and excess molar volumes in binary mixtures of cyclohexylamine + heptane, octane, nonane, decane, undecane, aniline, or water. *J. Chem. Eng. Data* **2006**, *51*, 176−180.

(27) Chen, J.-T.; Chang, W.-C. Excess molar volumes and viscosities for binary mixtures of cyclohexanone with methacrylic acid, benzyl methacrylate, and 2-hydroxyethyl methacrylate at (298.15, 308.15, and 318.15) K. *J. Chem. Eng. Data* **2006**, *51*, 88−92.

(28) Domańska, U.; Głoskowska, M. Experimental solid + liquid equilibria and excess molar volumes of alkanol + hexylamine mixtures: analysis in terms of the ERAS, DISQUAC, and Mod. UNIFAC models. *Fluid Phase Equilib*. **2004**, *216*, 135−145.

(29) Domańska, U.; Marciniak, M. Experimental (solid + liquid) and (liquid + liquid) equilibria and excess molar volume of alkanol + acetonitrile, propanenitrile, and butanenitrile mixtures. *J. Chem. Eng. Data* **2005**, *50*, 2035−2044.
(30) Kohler, F.; Liebermann, E.; Miksch, G.; Kainz, C. On the thermodynamics of the acetic acid−triethylamine system. *J. Phys. Chem.* **1972**, *76*, 2764−2768.
(31) Huang, X.; Margulis, C.; Li, Y.; Berne, B. J. Why is the partial molar volume of CO_2 so small when dissolved in a room-temperature ionic liquid? Structure and dynamics of CO_2 dissolved in [$bmim^+$][PF_6^-]. *J. Am. Chem. Soc.* **2005**, *127*, 17842−17851.
(32) Poling, B. E.; Prausnitz, J. M.; O'Connell, J. P. *The Properties of Gases and Liquids*, 5th ed.; McGraw-Hill: New York, 2000; pp 4.35, A.6, A.22.

Received for review June 16, 2006. Accepted July 17, 2006. The authors thank DuPont Central Research and Development for supporting the present work.

JE060275F